Sequence and pH Effects of LNA-Containing Triple Helix-Forming Oligonucleotides: Physical Chemistry, Biochemistry, and Modeling Studies[†,‡]

Bei-Wen Sun,[||] B. Ravindra Babu,[§] Mads D. Sørensen,[§] Krystyna Zakrzewska,[#] Jesper Wengel,[§] and Jian-Sheng Sun*[,⊥]

Laboratoire de Chimie Structurale et Spectroscopie Biomoléculaire, UMR7033 CNRS, UFR de Santé Medecine Biologie Humaine, Universite Paris-Nord, 93017 Bobigny Cedex, France, Nucleic Acid Center, Department of Chemistry, University of Southern Denmark, Campusvej 55, DK-5230 Odense M, Denmark, Laboratoire de Biochimie Theorique, UPR9080 CNRS, Institut de Biologie Physico-Chimique, 13 rue Pierre et Marie Curie, Paris 75005, France, and Laboratoire de Biophysique, USM 0503 ≪ Régulations et dynamique des génomes ≫, Muséum National d'Histoire Naturelle, UMR 5153 CNRS-MNHN, U 565 INSERM, 43 rue Cuvier 75231 Paris Cedex 05, France

Received November 18, 2003; Revised Manuscript Received February 5, 2004

ABSTRACT: Triple helix-forming oligonucleotides (TFOs) have been demonstrated to be capable of interfering with gene expression and modifying genomic DNA in a sequence-specific manner. Partial incorporation of 2′-*O*,4′-*C*-methylene linked locked nucleic acid (LNA) residues in TFOs has been shown to enhance significantly triple helix formation, whereas the full-length LNA TFO failed to form a stable triplex. This work is aimed at understanding the triple helix-forming properties of LNA-containing TFOs and at optimally designing their sequences. Both DNA thermal melting, gel retardation, and restriction enzyme experiments as well as modeling studies by molecular mechanics were carried out to investigate the base composition/sequence and pH-dependence effects of LNA-containing TFOs, as well as their structural features underlying triple helix formation. Alternating LNA substitution every 2−3 nucleotides in TFOs is mandatory, whereas the use of thymine LNA residues should be favored under neutral pH conditions. A rule for designing optimal LNA-containing TFOs is proposed. In addition, alternative LNA and 2′-*O*-methyl residues in TFOs do not significantly improve triple helix formation.

The design of molecules that can recognize specific sequences on the DNA double helix would provide interesting tools to manipulate DNA information processing at an early stage of gene expression and even to modify double-stranded DNA in a sequence-specific manner. The ability to interfere specifically with DNA metabolism has wide range of applications in functional biology and in gene-based biotechnology and therapeutics. It is an important challenge in biological and biomedical sciences. The so-called antigene strategy was first contemplated by two seminal works 15 years ago with the description of triple helix-forming oligonucleotides (TFOs) that can bind to the major groove of oligopyrimidine•oligopurine sequences in duplex DNA by hydrogen bonding with purine bases (*1*, *2*).

TFO-mediated inhibition of transcription has been reported in vitro and in cell cultures either through competition with the binding of transcription factors at promoter sites during the initiation stage or by arresting physically the transcription machinery during the elongation stage (*3*−*5*). The demonstration of the postulated triplex-mediated mechanism was provided by the use of mutant oligopyrimidine•oligopurine target sequences. The accessibility of TFOs to the transcriptionally active target genes under the chromatin environment was demonstrated by the use of psoralen−TFO or nitrogen mustard−TFO conjugates (*6*, *7*). The observation of triplex-mediated downregulation of expression of integrated genes into cellular chromosomes or endogenous genes on native chromosomes were additional proofs of TFOs' accessibility to their target sequences (*8*, *9*). Even though triplex formation is presently restricted to oligopyrimidine•oligopurine sequences, the fact that these sites can be located downstream of the transcription start site, including exons and introns, considerably increases the number of potential target genes for triplex-based strategies. In addition, activation of transcription has been achieved by using a triple helix-forming molecule (TFM) covalently tethered to activation domains (*10*). This suggests that a TFM−effector conjugate may be capable of selectively upregulating expression of a target gene, provided that the conjugates were appropriately designed and optimized. The approaches of triplex-mediated down- or upregulated gene expression of selectively targeted

[†] The Danish National Research Foundation and The Danish Research Agency provided financial support.

[‡] This work is dedicated to the memory of Professor Claude Hélène who inspired the studies of nucleic acids in the last two decades.

* To whom correspondence should be addressed. E-mail: sun@mnhn.fr; phone: 33 1 40793709; fax: 33 1 40793705.

[||] Universite Paris-Nord.

[§] University of Southern Denmark.

[#] UPR9080 CNRS, Institut de Biologie Physico-Chimique.

[⊥] Muséum National d'Histoire Naturelle, UMR 5153 CNRS-MNHN.

[1] Abbreviations: TFO, triple helix-forming oligonucleotide; TFM, triple helix-forming molecule; LNA, 2′-*O*,4′-*C*-methylene linked locked nucleic acid; T_m, melting temperature; UV, ultraviolet; •, Watson−Crick hydrogen bonding; x, Hoogsteen hydrogen bonding.

10.1021/bi036064e CCC: $27.50
Published on Web 03/20/2004

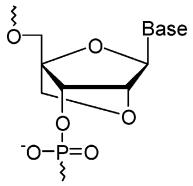

LNA

FIGURE 1: Chemical structure of 2′-*O*,4′-*C*-methylene linked LNA residues.

genes could be useful to dissect biological mechanisms and to alter phenotypes of cells and organisms.

During the past decade, many efforts have been devoted to modify TFOs to improve mostly binding properties to their cognate target sequences in a cellular environment. A number of chemically modified oligonucleotides have been shown to be active in cell cultures (see ref *11* for a recent review and the references therein) through antisense and/or antigene strategies. One of the promising modified oligonucleotides is locked nucleic acid (LNA) that can be considered as an analogue of an RNA derivative in which the ribose ring is constrained by a methylene linkage between the 2′-oxygen and the 4′-carbon (Figure 1). This bridge results in a locked C3′-endo sugar puckering and thus reduces the conformational flexibility of the ribose and increases the local organization of the phosphodiester backbone. This conformational restriction enhances binding affinity for complementary sequences with high sequence selectivity. It confers nuclease resistance but leads to an inability to activate RNase H for fully modified LNA (*12*−*16*). LNA−DNA chimera were used as antisense oligonucleotides to target a G-protein-coupled receptor and produced a physiologic response when injected directly into rats (*17*). Injection of LNA were well tolerated, suggesting that their in vivo toxicity is mild.

It has recently been shown that the (T,C)-motif TFOs partially substituted by LNA pyrimidines significantly enhance triple helix formation, whereas the same TFO sequence composed entirely of LNA residues failed to form a triplex (*18*, *19*). It seems thus that there is a balance between the preorganized strand conformation of the TFO owing to LNA residues and the necessary flexibility of the third strand to ensure optimal triple helix formation. The present work addresses this issue for a better understanding of triple helix-forming properties of LNA-containing TFOs and a better sequence design of these TFOs. To achieve these goals, both DNA melting experiments, biochemical assays, and molecular modeling studies have been carried out to study the base composition/sequence and pH-dependence effects of LNA-containing TFOs, as well as their structural features underlying triple helix formation. A rule for designing optimal LNA-containing TFOs will be proposed. In this manuscript, the symbols • and x designate Watson−Crick and Hoogsteen hydrogen bonding, respectively.

MATERIALS AND METHODS

Oligonucleotide and LNA Synthesis. Deoxyoligonucleotides were synthesized by Eurogentec (Seraing, Belgium), and used without further purification. LNA phosphoramidites were prepared as previously described (*13*). Synthesis of LNAs was performed in a 0.2 μmol scale on an automated DNA synthesizer using the phosphoramidite approach (*20*).

Table 1: Melting Temperature (T_m) of Triple Helices Studied in This Work[a]

Target double helix sequence:

3′-GGTGAAAAA**TTTTCTTTTCCCCCCT**GACC-5′
5′-CCACTTTTT**AAAAGAAAAGGGGGGA**CTGG-3′

TFO	Sequence	Tm (±1°C) pH 6.2	Tm (±1°C) pH 7.2
16TC	5′-TTTTCTTTTCCCCCCT-3′	18	~4
LNA1	5′-ttttCTTTTCCCCCCT-3′	22	n.d.
LNA2	5′-TtTtCtTtTCCCCCCT-3′	35	26
LNA3	5′-tTTtCtTtTCCCCCCT-3′	37	26
LNA4	5′-TTTTcTTTTcCcCcCT-3′	32	8
LNA5	5′-TTTtCTtTTcCCcCCT-3′	39	18
LNA6	5′-tTTtCTtTTcCCcCCT-3′	43	23
LNA7	5′-tTtTcTtTtT*c*C*c*C*c*T-3′	48	n.d.
LNA8	5′-t<u>T</u>t<u>T</u>c<u>T</u>t<u>T</u>t<u>C</u>c<u>C</u>c<u>C</u>cT-3′	51	n.d.

[a] The sequence of 29-bp double helices is shown on the top where the 16-bp target oligopyrimidine•oligopurine sequence is shown in bold. The melting experiments were carried out in 10 mM sodium cacodylate buffer at the indicated pH in the presence of 100 mM NaCl and 10 mM $MgCl_2$ (see Materials and Methods for experimental details). The concentration of duplex and TFOs were 1 and 1.5 μM, respectively. The symbols used for modified nucleotides are as follows: lower case letters t and c are LNA thymine and LNA 5-methycytosine, respectively; underlined upper case letters T and C are 2′-*O*-methyl,thymine and cytosine, respectively; italic upper case letter C is 5-methycytosine.

Standard procedures were used with modifications as described previously for the LNA phosphoramidites (6−10 min coupling time using "hand-couplings" and 1*H*-tetrazole or pyridine hydrochloride as activator) (*21*). Coupling yields >98% were obtained for LNA phosphoramidites and commercially available DNA amidites. Satisfactory purities (>80%) of the synthesized LNAs were verified by capillary gel electrophoresis and the compositions by MALDI-MS analysis. The matrix used for MALDI-TOF experiment is 3-hydroxypicolinic acid (50 mg/mL) mixed with ammonium citrate (10 mg/mL) dissolved in water/acetonitrile (1:1). The concentration of all oligonucleotides was determined from absorbance at 260 nm according to the nearest-neighbor model (*22*). A 29-bp double helix containing the 16-bp oligopyrimidine•oligopurine target sequence for triple helix formation was used (Table 1).

DNA Thermal Denaturation by UV Spectrophotometry. Thermal stability of triple helices was measured by a dual beam UV spectrophotometer. All the DNA thermal denaturation and renaturation experiments were performed on a UVIKON XL spectrophotometer equipped with a sample holder whose temperature was controlled by a Peltier device, and interfaced to a computer for experiment control, data acquisition, and analysis. Typically, the melting experiment started at 60 °C and decreased to 0 °C, and then increased back to 80 °C at a rate of 0.1°/min. Quartz cuvettes of 1-cm optical path length were used. The absorbance at 266 or 300

was recorded every 10 min. The sample temperature was measured by a Teflon-coated temperature probe immersed directly in a control cuvette. All the oligonucleotide samples were prepared in 10 mM sodium cacodylate buffer at pH 6.2 or 7.2 containing 100 mM sodium chloride and 10 mM magnesium chloride. A common pool of solution containing 1 μM target double helix was first prepared and then distributed into the cuvettes before mixing with 1.5 μM TFO. This protocol provides better sample preparation and makes differential melting experiments possible, if necessary. Differential melting experiments were carried out either by subtracting the duplex melting curve from the triplex one, or by placing the sample containing the duplex solution in the reference beam and that of triplex in the sample beam, to better determine the thermal duplex−triplex transition. The melting temperatures (T_m) were evaluated as the midpoint of the triple helix ↔ double helix + TFO transition of the melting curves. On the basis of multiple experiments, the uncertainty in T_m was estimated at ±1°C.

Gel Retardation Assay. A 29-bp double-stranded DNA fragment containing a 16-bp oligopyrimidine•oligopurine target sequence (Table 1) was radiolabeled at one 5′-end (20 nM) and was incubated in the presence of 1 μM TFO in 10 μlL of a solution containing 50 mM MES, pH 6.0, 100 mM NaCl, 10 mM $MgCl_2$, and 10% sucrose. After overnight incubation at a controlled temperature, samples were loaded on a 15% nondenaturing polyacrylamide (19:1) gel. Electrophoresis was performed in 50 mM MES, pH 6.0, and 10 mM $MgCl_2$ at 25 or 37 °C. After drying, the gel was exposed to a phosphorimager storage screen and quantification was performed on a Phosphorimager densitometer (Molecular Dynamics).

Restriction Enzyme Assay. A 6810-bp plasmid pLG containing the 16-bp oligopyrimidine•oligopurine target sequence was used as a substrate for the restriction enzyme Dra I. The cleavage reaction was performed in the presence of 1 μM TFOs at 25 °C during 15 min with 10 units of Dra I in a buffer containing 50 mM potassium acetate, 20 mM Tris-acetate, pH 7.9, 10 mM magnesium acetate, 0.5 mM spermine, and 1 mM dithiothreitol, after an overnight incubation. The reaction was stopped by the addition of 0.1 M EDTA. Samples were then loaded on a 0.8% nondenaturing agarose gel and stained by ethidium bromide dye for imaging.

Molecular Modeling. Molecular modeling by conformational energy-minimization was carried out using the *JUMNA* (version 10) program package (*23*), which allows the inclusion of virtually any modified nucleotides into the calculation via the *Nchem* utility program. The *Nchem* program was used both to calculate the partial charges and to evaluate the appropriate geometrical parameters for modified nucleotides, and prepare the file containing the information required by the *JUMNA* program. Nchem utilizes a *Huckel-Del Re* procedure for calculation of the partial atomic charges. Neither water nor positively charged counterions were explicitly included in the energy minimization. However, their effects were simulated by a sigmoidal, distance-dependent, dielectric function (*24*) and by assignment of a half negative charge for each phosphate group. Computations were carried out on a Pentium 4 PC under Linux.

The LNA residues were constructed by addition of a methoxy group at the 2′-deoxyribose position. The H4′ atom and one of the hydrogen of the methylene were declared as dummy atoms. The closure of the methylene with the 4′-C was performed by *JUMNA* program through a virtual bond with nominal C−C bond length, as well as angular and torsional angles by applying appropriate constraints during energy minimization.

Canonical coordinates of double helices (B80 and A80) were used for building double helices. The coordinates of triple helices were derived from the previously published B-like triple helix (*25*, *26*), which is consistent with NMR and vibrational spectroscopic studies. The helix length was 10 base pairs or base triplets. Appropriate constraints were applied to simulate sequence symmetry (cf. results for details).

RESULTS

Both experimental and computational approaches were performed to study the base composition/sequence and pH-dependence effects of the (T,C)-motif triple helix-forming oligonucletides (TFOs) which contain LNA residues, as well as their structural features underlying triple helix formation.

Melting Experiments. Melting experiments were carried out by using UV spectrophotometer to assess the thermal stability of triple helices. Eight LNA-containing TFOs were investigated to study the effects of base composition, sequence, and pH. Figure 2A shows the melting curves of the samples containing the target duplex and the TFOs (16TC, LNA3) as well as the duplex alone at pH 6.2 (recorded at 265 nm). The melting profiles of all samples were almost reversible when the heating and cooling rate was set at 0.1 °C/min, indicative of the equilibrium of reaction under the used experimental condition. The thermal transition at the high temperature (around 68 °C) was the same as that observed in the duplex sample, and thus was assigned to the double helix ↔ single strands transition. The thermal transition occurring at lower temperature in the samples containing both duplex and TFO was assigned to the triple helix ↔ double helix + TFO transition. It was noted that the melting transition of the triple helix LNA3 occurred at a higher temperature, but the transition was less pronounced in amplitude than that of the control triple helix with unmodified TFO (16TC). Because of less cooperative transition of the triple helix ↔ double helix transition of the triplexes made of LNA3 (and other LNA-containing TFOs, not shown), their T_m values were determined according to their melting profile recorded at 300 nm (Figure 2B) and were found identical within experimental error to that determined from their differential melting curves (Figure 2C, see Materials and Methods) It has been established that the change of absorbance at longer wavelengths (295−305 nm) indicates the formation of a nucleic acid structure which requires protonation/deprotonation of cytosines (*27*): at this wavelength, the spectral difference between protonated and nonprotonated cytosine is maximum, as inferred from absorbance spectra at different pH values. It was observed throughout this work that the triple helix ↔ double helix + TFO transition of all LNA-containing triple helices was less pronounced than that with unmodified TFO (16TC). This indicates that the formation of LNA-containing triple helices is less enthalpy driven than the unmodified triple helices.

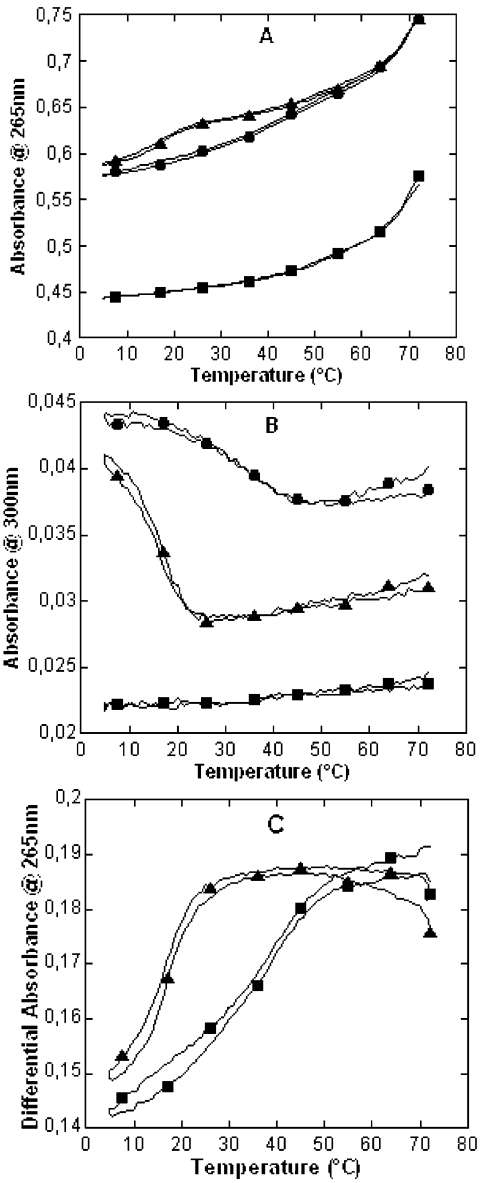

FIGURE 2: (A) Melting curves of the 29-bp double helix (filled squares) and the triple helices recorded at 266 nm: 16TC (filled triangles); LNA3 (filled circles); (B) melting curves of 29-bp double helix (filled squares) and the triplexes 16TC (filled triangles) and LNA2 (filled circles) recorded at the 300 nm (see text for details); (C) differential melting curves of the triple helices formed by 16TC (filled triangles) and LNA3 (filled squares) (see Materials and Methods for details). Experiments were carried out in 10 mM sodium cacodylate buffer at pH 6.2 in the presence of 100 mM NaCl and 10 mM $MgCl_2$. The concentration of duplex and TFOs were 1 and 1.5 μM, respectively.

The thermal stability as indicated by the T_m value of all triple helices is given in Table 1. At pH 6.2, it was found that the consecutive substitution of four thymines by their LNA analogues at the 5′-side of TFO had little stabilizing effect (1 °C/substitution, LNA1 vs 16TC), whereas alternating substitution by LNA strongly stabilized triple helices (about 4.5 °C/substitution, LNA2 or LNA3 vs 16TC). Alternating substitution of four cytosines by 5-methylcytosine LNA residues also has a notable triplex-stabilizing effect (3.5 °C/substitution, LNA4 vs 16TC), but less than thymine LNA. For the TFOs containing mixed thymine and 5-methylcytosine LNA, the T_m value of triple helices increased with the number of LNA residues (LNA5, LNA6, and LNA7).

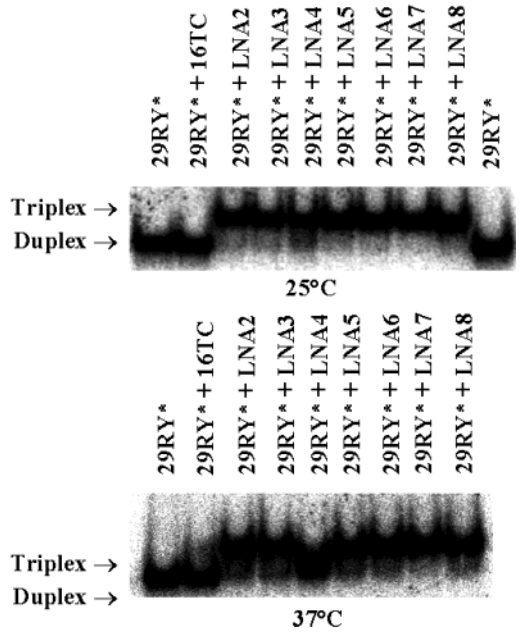

FIGURE 3: Gel retardation experiments were performed with 20 nM of radiolabeled duplex and 1 μM TFO in 50 mM MES, pH 6.0, 100 mM NaCl, 10 mM $MgCl_2$, and 10% sucrose at 25 °C (upper panel) and at 37 °C (lower panel) (see Materials and Methods for experimental details).

However, the extent of triplex stabilization per LNA substitution was greater for one LNA residue every three nucleotides (about 5 °C/LNA residue, LNA5 and LNA6) than one LNA every two nucleotides (about 3.8 °C/LNA residue, LNA7). It is worth noting that a mixed LNA and 2′-*O*-methyl TFO displayed only slightly higher triplex thermal stability than its LNA-containing analogue (LNA8 vs LNA7) under acidic conditions.

As expected, the thermal stability of all these (T,C)-motif triple helices was decreased when the pH was raised from 6.2 to 7.2, due to a lower degree of cytosine protonation. However, the pH dependence of these LNA-containing TFOs revealed some unusual features. At pH 7.2, the thermal stability of the triplexes formed by thymine LNA-containing TFOs (LNA2 and LNA3) was decreased by 8−11 °C. This triplex destabilization was notably less than that of all DNA TFOs (about −14 °C, 16TC). In contrast, the triplex formed by 5-methylcytosine LNA-containing TFO in the absence of thymine LNA was dramatically destabilized by 24 °C (LNA4). The same trend was observed for the mixed thymine and 5-methylcytosine LNA-containing TFOs (−21 °C, LNA5 and LNA6), but it is noted that the LNA-containing TFOs form much stable triplexes than the isosequential phosphodiester TFO (16TC) even at neutral pH. Our data were consistent with the previously published data (*19*). The observed variation of triplex stabilities of LNA-containing TFOs indicated a specific effect of the base composition of thymine and 5-methylcytosine LNA residues.

Gel Retardation Experiments. Gel retardation experiments were carried out in the presence of 1 μM TFOs under acidic conditions (pH 6.0). Figure 3 shows that the labeled 29-bp dsDNA fragment containing the 16-bp oligopyrimidine• oligopurine target sequence exhibited reduced electromobility in the presence of all LNA-containing TFOs, indicative of triple helix formation, except the unmodified TFO (16TC) at 25 °C. At 37 °C, partial dissociation of triplex was notably

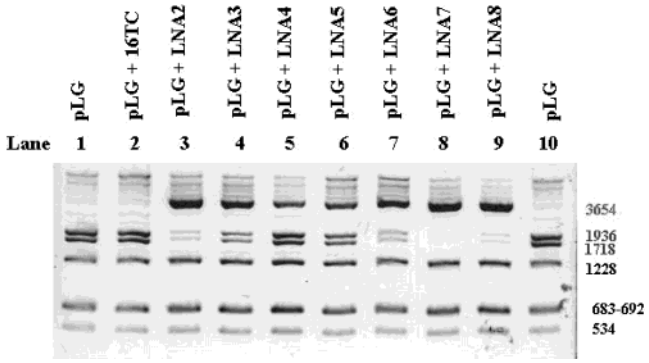

FIGURE 4: Dra I restriction enzyme assay was carried out with 0.5 μg of pLG plasmid and in the presence of 1 μM TFOs in 50 mM potassium acetate, 20 mM Tris-acetate, pH 7.9, 10 mM magnesium acetate, 0.5 mM spermine, and 1 mM dithiothreitol (see Materials and Methods for experimental details).

observed for LNA4 which contains only four 5-methylcytosine LNA residues. These data were consistent with T_m values measured at pH 6.2 (Table 1).

Restriction Enzyme Assays. The 16-bp oligopyrimidine•oligopurine target sequence provides a cleavage site for the restriction enzyme Dra I. This enzyme cleaves exactly at the 5′ junction of triple helix site (5′-TTT↓AAA-3′) and triple helix formation competes with the binding of Dra I and thus inhibits DNA cleavage (*28*). A plasmid (pLG) carrying one copy of 16-bp oligopyrimidine•oligopurine sequence was used as a substrate for the Dra I enzyme. The plasmide contains seven Dra I cleavage sites that generate DNA fragments of 19, 534, 683, 692, 1228, 1718, and 1936 bp. Inhibition of Dra I cleavage by triple helix formation leads to the disappearance of the 1718- and 1936-bp cleavage products and to the appearance of a 3648-bp fragment, while other DNA fragments were left unaffected which were used as internal controls. Figure 4 shows that, upon addition of 1 μM TFOs, all LNA-containing TFOs could inhibit Dra I cleavage with various efficiencies, but not the unmodified TFO (16TC) at 25 °C and pH 7.9. Complete inhibition was obtained with LNA7. The extent of Dra I inhibition was given as the following: LNA7 > LNA8 ≥ LNA2 ≈ LNA6 ≥ LNA3 ≥ LNA5 > LNA4 ≫ 16TC. These results were mainly consistent with the available T_m data at pH 7.2 (Table 1). It is noted that the alternating LNA and 2′-*O*-methyl TFO (LNA8) was slightly less potent than that of alternating LNA and DNA TFO (LNA7) at pH 7.9. The LNA4 which contains four 5-methylcytosine LNA residues was the least potent in inhibiting DNA cleavage by Dra I enzyme, except the unmodified TFO (16TC).

Modeling. Molecular modeling was carried out with the aim to delineate the molecular mechanics of double and triple helices where one strand contains LNA residues. The *JUMNA* program (*23*) was used due to its capacity to control helicoidal parameters throughout computation. Focus was made on the position/sequence effect of LNA residues. Therefore, the data are primarily shown on the duplex and triplex formed by homothymidylate and homoadenylate (cf. Tables 2 and 4).

Mononucleotide symmetry was applied when one strand was fully substituted by LNA residues as well as the unmodified control sequence (D1−2; R1−2; T1−2). Dinucleotide symmetry was used for alternatively substituted structures (D5−6; R5−6; T5−6). When a half part of helices

Table 2: Complexation Energy of Double-Stranded Complexes Studied in This Work[a]

	Duplex	ΔE_T	ΔE_A	E_{Inter} LJ	E_{Inter} Elec	E_C
D1	5′-TTTTTTTTTT-3′ 3′-AAAAAAAAAA-5′	+17.3	+30.8	-67.9	-99.6	-119.4
D2	5′-**t**t**t**t**t**t**t**t**t**t-3′ 3′-AAAAAAAAAA-5′	+11.2	+37.6	-76.4	-94.3	-121.9
D3	5′-**t**t**t**t**t**TTTTT-3′ 3′-AAAAAAAAAA-5′	+2.3	+37.8	-72.4	-93.5	-125.8
D4	5′-TTTTT**t**t**t**t**t**-3′ 3′-AAAAAAAAAA-5′	+10.9	+37.0	-71.0	-97.2	-120.3
D5	5′-t**t**T**t**T**t**T**t**T-3′ 3′-AAAAAAAAAA-5′	+11.7	+36.6	-74.7	-93.2	-119.6
D6	5′-T**t**T**t**T**t**T**t**T**t**-3′ 3′-AAAAAAAAAA-5′	+13.2	+36.3	-74.3	-93.1	-117.9
R1	5′-TTTTTTTTTT-3′ 3′-AAAAAAAAAA-5′	+16.7	+36.6	-68.1	-100.	-114.8
R2	5′-**t**t**t**t**t**t**t**t**t**t-3′ 3′-AAAAAAAAAA-5′	+13.5	+45.7	-79.2	95.6	-115.6
R3	5′-**t**t**t**t**t**TTTTT-3′ 3′-AAAAAAAAAA-5′	+5.5	+39.5	-73.7	-93.2	-121.9
R4	5′-TTTTT**t**t**t**t**t**-3′ 3′-AAAAAAAAAA-5′	+14.6	+39.9	-74.3	-92.3	-112.1
R5	5′-t**t**T**t**T**t**T**t**T-3′ 3′-AAAAAAAAAA-5′	+13.2	+39.3	-76.6	-93.5	-117.6
R6	5′-T**t**T**t**T**t**T**t**T-3′ 3′-AAAAAAAAAA-5′	+14.8	+39.0	-76.3	-93.5	-116.0

[a] The total complexation energy (E_C) was decomposed in terms of intermolecular interactions (E_{inter}) between the two strands in the double helix, as well as the conformational deformation energy of the individual strands (ΔE_T, ΔE_A) in the duplex (see text for details). LJ and Elec are Lenard-Jones and electrostatic components of interstrand interaction. Thymine-LNA residues are indicated by a bold lower case letter t. The RNA strand is given in underlined upper case letters. Energy is given in kcal mol^{-1}.

consecutively contained LNA residues (D3−4; R3−4; T3−4), the three last base pairs or triplets at both ends were restrained to mononucleotide symmetry to avoid end effects and to focus on the transition between LNA residues and unmodified nucleotides (the central four base pairs or triplets).

It should be pointed out that the ions and solvent effects were not comprehensively treated by this force field based simulation. Therefore, one should be cautious when comparing structures with significantly different chemical structures (i.e., D1 vs D2; D2 vs D3, etc.). However, energy comparison should be possible for similar chemical structures (i.e., D3 vs D4; D5 vs D6, etc.).

The total complexation energy (E_C) was decomposed in terms of intermolecular interactions (E_{inter} for duplexes, or E_{DH-III} for triplexes) between the two strands in double helix or the third strand (III) and the target double-helical (DH) DNA, as well as the conformational deformation energy of the individual strands in duplex (ΔE_T, ΔE_A) or the double helix (ΔE_{DH}) and the third strand (ΔE_{III}) in triplex. Confor-

Table 3: Helical and Conformational Parameters of Some Modeled Double and Triple Helices[a]

	Duplex/Triplex	Xdisp	Rise	Inc	Tip	Twist	Chi	Phase	Ampli
D1	5′-TTTTTTTTTT-3′	-2.6	3.2	7.9	-15.5	34.6	33.2	15.1	38.1
	3′-AAAAAAAAAA-5′	-2.4		27.2	-20.3		51.8	5.2	33.2
D2	5′-**tttttttttt**-3′	-5.6	3.8	-6.6	-12.5	28.2	10.4	6.0	63.2
	3′-AAAAAAAAAA-5′	-5.5		7.3	11.5		60.0	153.0	40.0
R1	5′-TTTTTTTTTT-3′	-2.6	3.3	7.8	-14.7	35.4	32.7	15.2	38.0
	3′-AAAAAAAAAA-5′	-2.3		33.1	-21.8		51.8	7.4	31.5
R2	5′-**tttttttttt**-3′	-6.4	3.5	-5.2	-6.7	27.3	9.0	6.0	63.4
	3′-AAAAAAAAAA-5′	-6.3		4.6	4.9		10.1	8.5	43.8
T1	5′-TTTTTTTTTT-3′	-3.8		-.2	2.4		59.1	148.3	40.2
	3′-AAAAAAAAAA-5′	-3.8	3.4	-1.7	1.3	31.0	58.8	146.3	40.6
	3′-TTTTTTTTTT-5′	-4.1		0.8	3.0		56.7	142.6	40.6
T2	5′-TTTTTTTTTT-3′	-4.2		-4.1	4.8		37.1	109.0	38.1
	3′-AAAAAAAAAA-5′	-4.2	3.7	-7.4	1.6	28.5	57.8	146.5	42.6
	3′-**tttttttttt**-5′	-5.0		-11.7	-9.7		9.0	4.9	62.9

[a] Thymine-LNA residues are indicated by a bold lower case letter t. The RNA strand is given in underlined upper case letters.

Table 4: Complexation Energy of Double-Stranded Complexes Studied in This Work[a]

	Triplex	ΔE_{DH}	ΔE_{III}	E_{DH-III} LJ	E_{DH-III} Elec	E_C
T1	5′-TTTTTTTTTT-3′ 3′-AAAAAAAAAA-5′ 3′-TTTTTTTTTT-5′	+24.8	+39.6	-101.3	-84.9	-121.8
T2	5′-TTTTTTTTTT-3′ 3′-AAAAAAAAAA-5′ 3′-**tttttttttt**-5′	+35.3	+10.3	-103.8	-76.4	-134.6
T3	5′-TTTTTTTTTT-3′ 3′-AAAAAAAAAA-5′ 3′-TTTTT**ttttt**-5′	+29.7	+18.0	-101.3	-83.6	-137.2
T4	5′-TTTTTTTTTT-3′ 3′-AAAAAAAAAA-5′ 3′-**ttttt**TTTTT-5′	+27.9	+20.9	-102.7	-78.8	-132.8
T5	5′-TTTTTTTTTT-3′ 3′-AAAAAAAAAA-5′ 3′-TtTtTtTtTt-5′	+27.9	+12.1	-102.8	-86.0	-148.8
T6	5′-TTTTTTTTTT-3′ 3′-AAAAAAAAAA-5′ 3′-tTtTtTtTtT-5′	+27.6	+13.3	-102.4	-85.4	-146.9

[a] The total complexation energy (E_C) was decomposed in terms of intermolecular interactions (E_{DH-III}) between the target double-helical DNA (DH) and the third strand (III), as well as the conformational deformation energy of the double helix (ΔE_{DH}) and the third strand (ΔE_{III}) in triplex (see text for details). LJ and Elec are Lenard-Jones and electrostatic components of intermolecular interaction. Thymine-LNA residues are indicated by a bold lower case letter t. Energy is given in kcal mol^{-1}.

mational deformation energies were evaluated as the difference between the corresponding energetic components before and after duplex or triplex formation. It should be noted that this evaluation is approximate, especially for the single strand since the conformation of a free single-stranded DNA is generally less well defined than a free double-stranded DNA. However, these approximations were necessary to take into account the effect of nucleotide modification.

(a) Double Helix. Six double helices made of decadeoxyriboadenylates and unmodified decadeoxyribo-thymidylates or LNA-containing decathymidylates were modeled (D1-D6, Table 2). Similar modeling was also performed on decarboadenylates (R1−R6, Table 2). Energy analysis of different structures is shown in Table 2. It was found that the full-length LNA substitution leads to stronger complexation with either deoxyriboadenylate (D2) or riboadenylate (R2) than do the unmodified complexes (D1 and R1, respectively). This was due to, in part, an increase of the interstrand interaction energy (LJ + Elec) which was mainly ascribed to the increase of hydrogen bonding (−18.1 kcal for D2 vs D1; −16.9 kcal for R2 vs R1, data not shown). It was also noted that the strand deformation energy was reduced for the LNA-containing thymidylate strand, whereas it was increased for the unmodified adenylate strand. Structural analysis (Table 3) shows significant changes in helical parameters upon binding of full-length LNA-containing thymidylate: (i) the base pairs were further displaced (3−4 Å) into the minor groove; (ii) significant rise increase; and (iii) reduced propeller twist. In addition, for LNA thymidylate residues, the glycosidic torsion adopted a high anti conformation, and the sugar puckering was at C3′-endo conformation with an unusual high amplitude (about +50% as compared to unmodified sugar).

The duplexes D3 and D4 (also R3 and R4) were modeled to study the effect of transition between LNA residues and oligodeoxynucleotide (DNA). It turned out that, in all cases, the duplexes D3 and R3 had lower complexation energy than

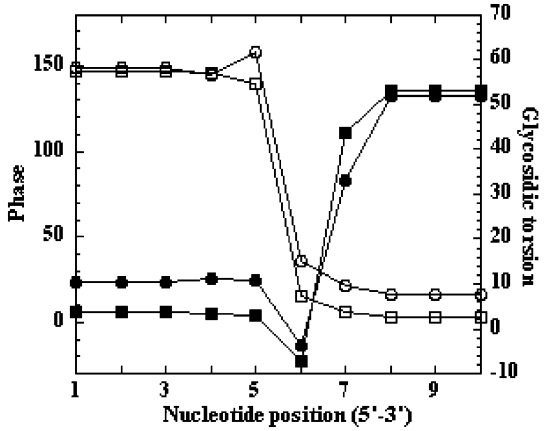

FIGURE 5: Plots of phase of sugar puckers (squares) and glycosidic torsion (circles) in the triplexes T3 (filled symbols) and T4 (open symbols) (see text for details).

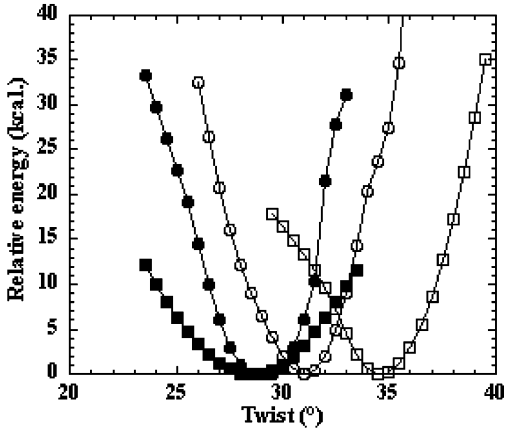

FIGURE 6: Twist adiabatic mapping of the duplex D1 (open squares) and D2 (filled squares) and the triplex T1 (open circles) and T2 (filled circles) (see text for details).

the duplexes D4 and R4, respectively. Thus, it indicated that a LNA5′-3′DNA step is energetically more favored than a DNA5′-3′LNA step. For the alternately substituted duplex, the duplexes D5 and R5, which had one more LNA5′-3′DNA step than DNA5′-3′LNA step, were more stable than the duplexes (D6 and R6) with one more DNA5′-3′LNA step. In addition, it was noted that the presence of the LNA residue at the 5′-side constrained the DNA residue at its 3′-side to adopt the C3′-endo conformation (data not shown) as reported in our previous NMR studies (*29*, *30*).

(b) Triple Helix. Similar to the duplex studies, six triple helices were modeled and their energies were analyzed (Table 4). It was found that the triplex with full-length LNA TFO (T2) had reduced interstrand interaction energy mainly due to the electrostatic component as compared to that of the triplex (T1). The deformation energy of the LNA strand was considerably reduced, whereas that of the target duplex was significantly increased. As observed in LNA-containing duplex, the base triplets were further displaced into the minor groove and the rise was slightly increased with associated reduction in twist (Table 3). The LNA thymines in the third strand adopted high anti conformation with C3′-endo and high amplitude sugar puckering.

As observed in the duplex, the triplex with only one LNA5′-3′DNA step in the third strand (T3) was energetically more favored than that with one DNA5′-3′LNA step (T4). This observation was also confirmed with alternately substituted LNA (T5 vs T6). It was noted that the triplexes where the third strand is made of alternating LNA residues (T5 and T6) had the strongest interaction energy (LJ + Elec) and the smallest DNA deformation energy (ΔE_{DH} and ΔE_{III}).

Figure 5 shows the variation of the sugar pucker phase and the glycosidic torsion along the third strand containing five consecutively substituted LNA (T3 and T4). It was found that the transition from a tract of LNA located at the 5′-side to that of ODN at the 3′-side exceeded one more nucleotide at the 3′-side and two nucleotides were likely necessary for the transition. However, the transition involving a tract of ODN at the 5′-side and that of LNA at the 3′-side almost took place at the junction.

(c) Helical Flexibility. The deformability/flexibility of the duplexes and triplexes containing a full-length substituted LNA strand was assessed by mapping of the twist around the energy minimized structure in a step-to-step manner. Constraint on the twist was set with a step of 1° and then the energy minimization was performed. Figure 6 shows that stable energy wells were obtained, which indicated that the energy-minimized structures were quite stable. Unexpectedly, the duplex D2 was about 2-fold more flexible than the unmodified duplex D1 (this observation holds true for the duplex R2 vs R1, data not shown). The triplex containing full-length substituted LNA TFO has considerably reduced twist flexibility as compared to the duplex D2, but was slightly more flexible than the unmodified triplex T1.

DISCUSSION

Combined experimental and modeling studies consistently point to the following characteristic features of the (T,C)-motif triple helix formation where the TFO contains LNA residues. It should be kept in mind that the energy calculations by conformational energy minimization in this work were indicative, as the ionic and hydration effects were not explicitly treated in these molecular mechanics calculations. However, the results provide an important qualitative perception of the general energetic contribution of the systems and insights to possible explanation of their physical chemistry and structural properties.

Structure and Energy Consideration, Sequence Effect. One of the main characteristics of all structures, either double helices (LNA•DNA, LNA•RNA) or triple helices (DNA•DNAxLNA), where one strand contains LNA residues, is the rather far displacement of bases of the LNA-containing strand in the minor groove and high rise values as compared to their DNA analogues. They are the direct consequence of the 2′-*O*,4′-*C*-methylene-linked sugar: the unusual high puckering amplitude (about +50%) of LNA residue almost excludes effective base stacking if base pairs remained at the center of helical axis. Therefore, the base pairs have to move further away into the minor groove to avoid steric hindrance between base and sugar moieties and to ensure base stacking which is still less important (mainly originating from less interstrand stacking) than in unmodified structures. It can also explain the higher twist helical flexibility in duplex D2 (but also R2, data not shown), and to a less extent, in triplex T2 as compared to the duplex D1 (and R1) and the triplex T1, respectively. In double helices, the reduced propeller twist observed in all duplexes containing LNA residues can account for the increase in hydrogen

bonding which compensated, in part, for the reduced base stacking. As anticipated, the deformation of the LNA-containing strand was significantly less important than deformation of the unmodified strand as a result of strand preorganization. On the other hand, the deformation energy of the pairing strand (dA_{10} or rA_{10}) or double helix (T_{10}•A_{10}) was higher upon binding of the LNA-containing strand. In particular, the deformation energy cost of double helix may explain: (i) the reported observation that a full-length LNA residue TFO was unable to form stable triple helix (*14*); (ii) the partial consecutive substitution of DNA thymines by their LNA analogues had marginal effect on triplex stabilization as observed in the triplex LNA1 in the present study.

Further analyses show also that a LNA5′-3′DNA step is energetically favored with respect to a DNA5′-3′LNA step in all modeled double and triple helices with alternating DNA and LNA sequence (D3 vs D4, R3 vs R4 in Table 2; T3 vs T4 in Table 4, etc.). In addition, the complexes with one alternating strand of LNA and DNA residues have the strongest interstrand interaction (LJ + Elec). In particular, the triplexes where the third strand is made of full-length alternating LNA and DNA residues (Table 4, T5 and T6) have not only the strongest interstrand interaction but also the smallest double helix and the third strand deformation energy (ΔE_{DH} and ΔE_{III}). The experimental data in Table 1 were consistent with these predictions: the T_m value of the triplex LNA3 which had one DNA5′-3′LNA step less than the triplex LNA2 was +2 °C higher at pH 6.2, and they were higher than that of the triplex LNA1.

Taken together, the results of energy calculation consistently explain the observed T_m data listed in Table 1 and also the data in the literature (*18*, *19*). For instance, the preorganized LNA-containing TFOs and less important interstrand base stacking in LNA-containing triple helices would be consistent with the spectroscopic observation of melting profiles of these triplexes where their triple helix ↔ double helix + TFO transition was less pronounced than that with unmodified TFO (16TC), indicative of their more entropy-driven (or less enthalpy-driven) nature of triplex formation than the unmodified triple helices.

As pointed out above, the unusually high amplitude of sugar puckering (about +50%) of LNA residues is due to its short 2′-*O*,4′-*C*-methylene bridge. It can be expected that a longer bridge such as 2′-*O*,4′-*C*-ethylene (*31*) could reduce its puckering amplitude while keeping a locked C3′-endo conformation. In return, it could be achieved a better base stacking interaction and even allow full-length substituted TFO for triple helix formation. In the course of this manuscript preparation, a very recent report showing that a TFO with full-length 2′-*O*,4′-*C*-ethylene residues can indeed form stable triple helix (*32*) supports this inference.

Inspection of the triple-helical structures reveals also a clear difference between the triplex T2 formed by a full-length LNA TFO and the triplex T1 formed by unmodified TFO can be seen in Figure 7. The 2′-*O*,4′-*C*-methylene bridge in LNA TFO fills the narrow and shallow groove between TFO and the oligopurine strand. This could explain the property of LNA-containing TFO to enhance greatly triple helix formation as compared to the unmodified TFO, due to the additional release of water molecules and ions which could bind in this groove in the absence of LNA residues.

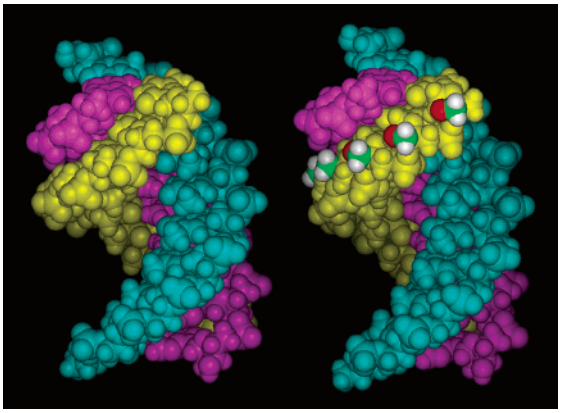

FIGURE 7: Space-filled models of the triplex T1 (left) and T2 (right). The models are slightly forward tilted. Oligopyrimidine and oligopurine strands are in blue and purple, respectively. TFO is in yellow. 2′-*O*,4′-*C*-Methylene bridge is in atom color.

Table 5: Variation of T_m Values Per +1 pH Unit (pH Dependence) of LNA-Containing TFOs Studied in This Work and in Other Works[a]

TFO	sequence	ΔT_m (°C)/ +1 pH unit	ref
16TC	5′-TTTTCTTTTCCCCCCT-3′	-14	this work
LNA2	5′-TtTtCtTtTCCCCCCT-3′	-9	this work
LNA3	5′-tTTtCtTtTCCCCCCT-3′	-11	this work
LNA4	5′-TTTTcTTTTcCcCcCT-3′	-24	this work
LNA5	5′-TTTtCTtTTcCCcCCT-3′	-21	this work
LNA6	5′-tTTtCTtTTcCCcCCT-3′	-20	this work
BNA-4	5′-tCtCtCtCcCtTTT-3′	-28	19, 32
BNA-5	5′-TcTcTcTcCcTtTT-3′	-37	19, 32

[a] Lower case letters t and c are LNA thymine and LNA 5-methylcytosine, respectively.

pH Dependence. Table 5 shows the variation of T_m values per +1 pH unit (pH dependence) of LNA-containing TFOs studied in this work and in other works. It seems that this variation relates to the nature of LNA residues, thymine and 5-methylcytosine. The pH dependence of (T,C)-motif TFOs originates from the protonation state of cytosines. Therefore, it can be reasonably assumed that the pH effect of a given TFO depends on its content of cytosine and the extent of pH effect of a given TFO could be additive for each of the cytosines. On the basis of this assumption and the observation that the thermal stability of the control DNA triplex (16TC) was decreased by about −14 °C upon the increase of one pH unit (from pH 6.2 to pH 7.2), it seems that, at least for the sequence studied in this work, the pH dependence of each DNA cytosine was −2 °C/pH. With these in mind, the observation of pH dependence of different triplexes can be analyzed as below.

The presence of four LNA-thymine in TFOs conferred the least destabilization of triplexes (LNA2 and LNA3) upon raising of one pH unit. The apparent pH dependence of each DNA cytosine was about −1.4 °C/pH in average. It seems that the enhanced triplex stability provided by LNA-thymine compensates in part the pH sensitivity of DNA cytosines.

The presence of four 5-methylcytosine LNA in the absence of thymine LNA residues in TFO dramatically destabilized the triplex (LNA4) by 24 °C/pH. Similar trend of pH dependence was observed in the triplexes made of mixed LNA thymines and LNA 5-methylcytosines in TFO (LNA5 and LNA6). However, even with only LNA 5-methylcytosine

substitution (LNA4), it had slightly higher thermal stability than the unmodified TFO (16TC) at pH 7.2.

The substitution of seven DNA cytosines in the control DNA triplex (16TC) by their 5-methyl analogues had marginal stabilizing effect (+4 °C at pH 6.2, data not shown) and the previous work showed that it did not change the pH dependence of TFO (*28*). Furthermore, Imanishi's group had reported that the substitution of cytosine in a TFO by either 5-methycytosine LNA or cytosine LNA exhibited the similar pH dependence (*19*, *32*). Therefore, it looks unlikely that the presence of 5-methyl group in the 5-methylcytosine LNA residues can account for its high sensitivity to pH change.

It is also unlikely that the high pH dependence of the 5-methylcytosine LNA residues observed in this work could be ascribed to this particular sequence which contains a tract of six cytosines in TFOs, as similar effect was also observed by Imanishi's group worked on a quite different sequence with many isolated cytosines. Especially, two isosequential TFOs with different content of 5-methylcytosine LNA residues exhibited significantly different pH dependence: −28 °C/pH unit for 5′-tCtCtCtCcCtTTT-3′ (BNA-4) and −37 °C/pH for 5′-TcTcTcTcCcTtTT-3′ (BNA-5) (*19*,*32*).

Energy calculations were carried out with the triplexes made of 10 C•GxC triplets where the cytosines in the third strand were either in their protonated or unprotonated state and the third strand was either full DNA or full LNA. It was found that the difference in complexation energy of the triplexes between the protonated and the unprotonated state of cytosines was roughly two times bigger when the third strand was LNA than DNA (data not shown). This could explain the observed high pH dependence of LNA 5-methylcytosine. Again, the reduced base stacking in triplex as a result of high sugar puckering of LNA residue could account for, at least in part, this weak withstanding to pH change.

Rules for Designing TFO Sequence. The data presented in this work and in the literature have shown that the sequence effect and the differential stabilization by thymine LNA and 5-methylcytosine LNA residues. These peculiar properties of LNA-containing TFOs dictate the following rules that should be useful for optimally designing the sequence of TFOs:

(i) Choose alternating LNA and DNA residues in TFO (e.g., use one LNA every two or three nucleotides)

(ii) Maximize the number of LNA5′-3′DNA steps in TFO (e.g., use one LNA residue at the 5′-end of TFO, when appropriate)

(iii) Maximize the use of thymine LNA residues

In summary, the present work shows that the stability of (T,C)-motif triple helices can be enhanced by substitution of 2′-deoxynucleotides by LNA residues every 2−3 nt in TFOs, in preference by LNA thymines, according to the proposed rules. It is also worth to note that TFO made of alternative LNA and 2′-*O*-methyl residues does not significantly improve triple helix formation. Further developments of LNA TFO derivatives should provide an exciting chemical approach for the control of gene expression and for a broad range of biotechnological and therapeutical applications.

ACKNOWLEDGMENT

Dr. Richard Lavery is acknowledged for helpful discussion about modeling of LNA-containing oligonucleotides. Ms. Britta M. Dahl is thanked for oligonucleotide synthesis and Dr. Michael Meldgaard, Exiqon A/S for MALDI-MS analyses.

REFERENCES

1. Le Doan, T., Perrouault, L., Praseuth, D., Habhoub, N., Decout, J. L., Thuong, N. T., Lhomme, J., and Hélène, C. (1987) Sequence-specific recognition, photocrosslinking and cleavage of the DNA double helix by an oligo-[alpha]-thymidylate covalently linked to an azidoproflavine derivative. *Nucleic Acids Res. 15*, 7749−7760.
2. Moser, H. E., and Dervan, P. B. (1987) Sequence-specific cleavage of double helical DNA by triple helix formation. *Science 238*, 645−650.
3. Escude, C., Giovannangeli, C., Sun, J. S., Lloyd, D. H., Chen, J. K., Gryaznov, S. M., Garestier, T., and Hélène, C. (1996) Stable triple helices formed by oligonucleotide N3′→P5′ phosphoramidates inhibit transcription elongation. *Proc. Natl. Acad. Sci. U.S.A.* 93, 4365−4369.
4. Grigoriev, M., Praseuth, D., Guieysse, A. L., Robin, P., Thuong, N. T., Hélène, C., and Harel-Bellan, A. (1993) Inhibition of interleukin-2 receptor alpha-subunit gene expression by oligonucleotide-directed triple helix formation. *C. R. Acad. Sci. III 316*, 492−495.
5. Ritchie, S., Boyd, F. M., Wong, J., and Bonham, K. (2000) Transcription of the human c-Src promoter is dependent on Sp1, a novel pyrimidine binding factor SPy, and can be inhibited by triplex-forming oligonucleotides. *J. Biol. Chem. 275*, 847−854.
6. Giovannangeli, C., Diviacco, S., Labrousse, V., Gryaznov, S., Charneau, P., and Hélène, C. (1997) Accessibility of nuclear DNA to triplex-forming oligonucleotides: the integrated HIV-1 provirus as a target. *Proc. Natl. Acad. Sci. U.S.A. 94*, 79−84.
7. Belousov, E. S., Afonina, I. A., Kutyavin, I. V., Gall, A. A., Reed, M. W., Gamper, H. B., Wydro, R. M., and Meyer, R. B. (1998) Triplex targeting of a native gene in permeabilized intact cells: covalent modification of the gene for the chemokine receptor CCR5. *Nucleic Acids Res. 26*, 1324−1328.
8. Faria, M., Wood, C., White, M., Hélène, C., and Giovannangeli, C. (2000) Targeted inhibition of transcription elongation mediated by triplex-forming phosphoramidate oligonucleotides. *Proc. Natl. Acad. Sci. U.S.A. 97*, 3862−3867.
9. Bailey, C., and Weeks, D. L. (2000) Understanding oligonucleotide-mediated inhibition of gene expression in *Xenopus laevis* oocytes. *Nucleic Acids Res. 28*, 1154−1161.
10. Kuznetsova, S., Ait-Si−Ali, S., Nagibneva, I., Troalen, F., Le Villain, J. P., Harel-Bellan, A., and Svinarchuk, F. (1999) Gene activation by triplex-forming oligonucleotide coupled to the activating domain of protein VP16. *Nucleic Acids Res. 27*, 3995−4000.
11. Sun, J. S., and Hélène, C. (2003) Oligonucleotides and derivatives as gene-specific control agents. *Nucleosides Nucleotides Nucleic Acids 22*, 483−499.
12. Singh, S. K., Nielsen, P., Koshkin, A. A., and Wengel, J. (1998) LNA (locked nucleic acids): synthesis and high-affinity nucleic acid recognition. *Chem. Commun.* 455−456.
13. Koshkin, A. A., Singh, S. K., Nielsen, P., Rajwanshi, V. K., Kumar, R., Meldgaard, M., Olsen, C. E., and Wengel, J. (1998) LNA (Locked Nucleic Acids): Synthesis of the adenine, cytosine, guanine, 5-methylcytosine, thymine and uracil bicyclonucleoside monomers, oligomerisation, and unprecedented nucleic acid recognition. *Tetrahedron 54*, 3607−3630.
14. Obika, S., Nanbu, D., Hari, Y., Andoh, J., Morio, K., Doi, T., and Imanishi, T. (1998) Stability and structural featrues of the duplexes containing nucleoside analogues with a fixed N-type conformation, 2′-*O*,4′-*C*-methyleneribonucleosides. *Tetrahedron Lett. 39*, 5401−5404.
15. Wengel, J. (1999) Synthesis of 3′-*C*- and 4′-*C*-branched oligodeoxynucleotides and the development of locked nucleic acid (LNA). *Acc. Chem. Res. 32*, 301−310.
16. Braasch, D. A., and Corey, D. R. (2000) Locked nucleic acids (LNA): fine-tuning of the recognition of DNA and RNA. *Chem. Biol. 8*, 1−7.
17. Wahlestedt, C., Salmi, P., Good, L., Kela, J., Johnsson, T., Hökfelt, T., Broberger, C., Porreca, F., Lai, J., Ren, K., Ossipov, M., Koshkin, A., Jabobsen, N., Skouv, J., Derum, H., Jacobsen, M. H., and Wengel, J. (2000) Potent and nontoxic antisense oligo-

nucleotides locked nucleic acids. *Proc. Natl. Acad. Sci. U.S.A. 97*, 5633−5638.
18. Torigoe, H., Hari, Y., Sekiguchi, M., Obika, S., and Imanishi, T. (2001) 2′-O,4′-C-methylene bridged nucleic acid modification promotes pyrimidine motif triplex DNA formation at physiological pH: thermodynamic and kinetic studies. *J. Biol. Chem. 276*, 2354−2360.
19. Obika. S., Uneda, T., Sugimoto, T., Nanbu, D., Minami, T., Doi, T., and Imanishi, T. (2001) 2′-O,4′−C-Methylene bridged nucleic acid (2′,4′-BNA): synthesis and triplex-forming properties. *Bioorg. Med. Chem. 9*, 1001−1011.
20. Caruthers, M. H. (1991) Chemical synthesis of DNA and DNA analogues. *Acc. Chem. Res. 24*, 278.
21. Rajwanshi, V. K., Håkannson, A. E., Dahl, B. M., and Wengel, J. (1999) LNA stereoisomers: *xylo*-LNA (*β*-D-*xylo* configured locked nucleic acid) and α-L-LNA (α−L-ribo configured locked nucleic acid). *Chem. Commun*. 1395−1396.
22. Cantor, C. R., Warshaw, M. M., and Shapiro, H. (1970) Oligonucleotide interactions. III. Conformational differences between deoxy- and ribodinucleoside phosphates. *Biopolymers 9*, 1059−1077.
23. Lavery, R., and Sklenar, H. (1988) The definition of generalized helicoidal parameters and of axis curvature for irregular nucleic acids. *J. Biomol. Struct. Dyn. 6*, 63−91.
24. Lavery, R., Sklenar, H., Zakrzewska, K., and Pullman, B. (1986) The flexibility of the nucleic acid: (I) "SIR", a novel approach to the variation of polymer geometry in constrained systems. *J. Biomol. Struct. Dyn. 3*, 989−1014.
25. Ouali, M., Letellier, R., Adnet, F., Liquier, J., Sun, J. S., Lavery, R., and Taillandier, E. (1993) A possible family of B-like triple helix structures: comparison with the Arnott A-like triple helix. *Biochemistry 3*, 2098−2103.
26. Ouali, M., Letellier, R., Sun, J. S., Akhebat, A., Adnet, F., Liquier, J., and Taillandier, E. (1993) Determination of G*G•C Triple Helix Structure by Molecular Modeling and Vibrational Spectroscopy. *J. Am. Chem. Soc. 115*, 4264−4270.
27. Mergny, J. L., and Lacroix, L. (1998) Kinetics and thermodynamics of i-DNA formation: phosphodiester versus modified oligodeoxynucleotides. *Nucleic Acid Res. 26*, 4797−4803.
28. Giovannangeli, C., Rougee, M., Garestier, T., Thuong, N. T., and Helene, C. (1992) Triple-helix formation by oligonucleotides containing the three bases thymine, cytosine, and guanine. *Proc. Natl. Acad. Sci. U.S.A. 89*, 8631−8635.
29. Petersen, M., Nielsen, C. B., Nielsen, K. E., Jensen, G. A., Bondensgaard, K. Singh, S. K., Rajwanshi, V. K., Koshkin, A. A., Dahl, B. M., Wengel, J., and Jacobsen, J. P. (2000) The conformations of locked nucleic acids (LNA). *J. Mol. Recognit. 13*, 44−53.
30. Petersen, M., Bondensgaard, K., Wengel, J., and Jacobsen, J. P. (2002) Locked nucleic acid (LNA) recognition of RNA: NMR solution structures of LNA: RNA hybrids. *J. Am. Chem. Soc. 124*, 5974−5982.
31. Morita, K., Takagi, M., Hasegawa, C., Kaneko, M., Tsutsumi, S., Sone, J., Ishikawa, T., Imanishi, T., and Koizumi, M. (2003) Synthesis and properties of 2′-*O*,4′-*C*-ethylene-bridged nucleic acids (ENA) as effective antisense oligonucleotides. *Bioorg. Med. Chem. 11*, 2211−2226.
32. Koizumi, M., Morita, K., Daigo, M., Tsutsumi, S., Abe, K., Obika, S., and Inanishi, T. (2003) Triplex formation with 2′-O,4′-C-ethylene-bridged nucleic acids (ENA) having C3′-endo conformation at physiological pH. *Nucleic Acid Res. 31*, 3267−3273.

BI036064E